EPJ Web of Conferences **21**, 08004 (2012)
DOI: 10.1051/epjconf/20122108004

Analysis of the (n,f) Reaction in the Plutonium Isotopes

Olivier Bouland[1,a], J.Eric Lynn[2], and Patrick Talou[2]

[1] Physics Studies Laboratory, CEA, DEN, DER, SPRC, Cadarache, F-13108 Saint-Paul-lez-Durance.
[2] T-2 Nuclear Theory Group, Los Alamos National Laboratory, Los Alamos, NM 87545, USA.

Abstract. This paper describes the modified Hauser-Feshbach formalism used to compute accurately fission cross sections for low-energy neutrons (from a few keV up to 5.5 MeV) in presence of intermediate structure in the second well. Application to the large plutonium isotope family (236 to 244) has been made with in particular reliable predictions of the cross sections of the short-lived nuclides. Special attention is paid to the choice of the model parameters entering in the calculations.

1 Introduction

The decay of a compound nucleus by fission is a complex multi-dimensional problem, whose description still requires many model parameters. The elucidation and physical understanding of these parameters is an ongoing research process, and this paper reports our progress in the study of the fission cross-sections for a long sequence of plutonium isotopes. Our ultimate goal is to replace many fitting parameters ubiquitous in current data evaluations with physically sound theory with fewer parameters. If successful, such an approach would lead to reliable predictions of the fission cross-sections of nuclides for which measurements are unavailable or very poor, while at the same time deepen our understanding of the fission process.

Here we present results obtained with a modern version of the AVXSF code (AVerage Cross Section of Fission), which treats in great detail the intermediate structure due to the presence of a second well on the fission path. The correct modeling of the class-II states properties and in particular, their coupling with the levels present in the first well as well as to the continuum, is crucial to infer meaningful barrier heights. Experimentally, those barrier heights can be inferred from an analysis of low-energy neutron-induced fission cross sections in the case of fertile nuclei, and transfer reactions leading to fission, e.g., (t, pf), in the case of fissile nuclei. The AVXSF code can treat both situations adequately in order to extract fission barrier heights.

In the following, the theory and main equations implemented in the AVXSF code are introduced. Approximate formulae valid in specific situations are also discussed. A Monte Carlo option is used when analytic approximations fail and a full sampling of the level characteristics distributions is needed. We then present preliminary results on the neutron-induced fission cross sections obtained for a suite of plutonium isotopes, for which a consistent set of model input parameters was developed. Our analysis encompasses neutron incident energies from a few keV up to 5.5 MeV, just below the onset of second-chance fission. The importance of fission barrier heights, nucleon pairing gaps and level densities is emphasized. This paper concludes on some examples of predicted cross sections with some reliability for the short-lived nuclides of the Pu series.

[a] e-mail: olivier.bouland@cea.fr

2 Theoretical Background

2.1 Hauser-Feshbach Theory.

The central postulate of the compound nucleus theory, the independence of formation and decay, is embodied in the Hauser-Feshbach formula [1] for average reaction cross-sections. In this a factor for the magnitude of the partial wave, embodying energy and spin-coupling factors, is multiplied by the product of transmission coefficients for the entrance and exit channels divided by the sum of transmission coefficients for all open channels. The individual transmission coefficients are envisaged as having a factor expressing the fraction of the internal nuclear wave-function near the compound nucleus surface being in the configuration of the channel and a factor expressing the penetrability of this component across the nuclear surface and through any external potential barriers in the channel. The same Hauser-Feshbach expression can be obtained by averaging over the Breit-Wigner single level formula describing the "microscopic" behaviour of the cross-section. This latter derivation shows that the transmission coefficient can be related to the ratio (the strength function) of the partial width for the channel to the level spacing of the resonances. This derivation gives the Hauser-Feshbach formula exactly if the partial widths are uniform from resonance to resonance. The highly fluctuating behaviour of the partial widths (described by the Porter-Thomas distribution [2]) implies that the Hauser-Feshbach formula is not exact and in practical use it is multiplied by a "fluctuation averaging" factor. When many channels are open this can be reduced to a one-dimensional numerical integral [3] denoted in this paper as S (with subscripts denoting entrance and exit channel, as necessary) . Other complications arise when the average partial widths approach or exceed the level spacing. In this case the relation of the transmission coefficient to the strength function becomes more complicated [4].

2.2 Inclusion of fission in Hauser-Feshbach theory.

Fission can be accommodated straightforwardly within this framework if the fission barrier is single humped. A very heavy nucleus is inherently unstable towards fission and since the whole nucleus is undergoing prolate deformation towards the scission point the fission transmission coefficient is governed solely by the penetrability through the fission barrier, which, in the liquid drop model, is governed by the constraining effect of the 'surface tension' forces on the repelling Coulomb forces. The Hill-Wheeler formula [5] for the transmission of a wave through a barrier of inverted harmonic oscillator form is normally used for this penetrability factor. As the deforming nucleus passes through this barrier it will be in a specific state of 'internal' excitation energy, the 'internal' degrees of freedom comprising collective degrees of freedom other than prolate deformation as well as nucleon degrees of freedom. This state of internal excitation reduces the energy available for deformation and this energy deficit is included in the Hill-Wheeler penetrability factor. The overall fission transmission coefficient is the sum of all the non-negligible penetrability factors for the various intrinsic states at the barrier.

Within a strict reaction theory, such as R-matrix theory, fission comprises a very large number of channels, which are formally defined at or beyond the scission point as the incipient fission product pairs in a multitude of states of excitation energy and angular momentum relationships. This gives rise to the expectation that the total fission width should be nearly uniform from resonance to resonance, just as total radiation widths are. However, A. Bohr [6] showed that important post-scission behaviour aspects of the fission products, such as overall angular distribution, are dependent on the state of intrinsic excitation at the saddle point and proposed that these intrinsic states (henceforward referred to also as transition states) should be regarded as the 'physical' channels. The fact that experimental measurements of fission widths in the resonances of fissile nuclei showed that they fluctuate widely from resonance to resonance reinforced this point of view. In fact, the fission widths at the scission point are all correlated with each other to the extent that their common derivation is from a single transition state. We therefore have the concept of a barrier channel for each transition state, each is associated with its own mean width, or, equivalently, strength function (given by the Hill-Wheeler factor) and Porter-Thomas distribution, and they can be included as such in the Dresner integral for the fluctuation averaging factor.

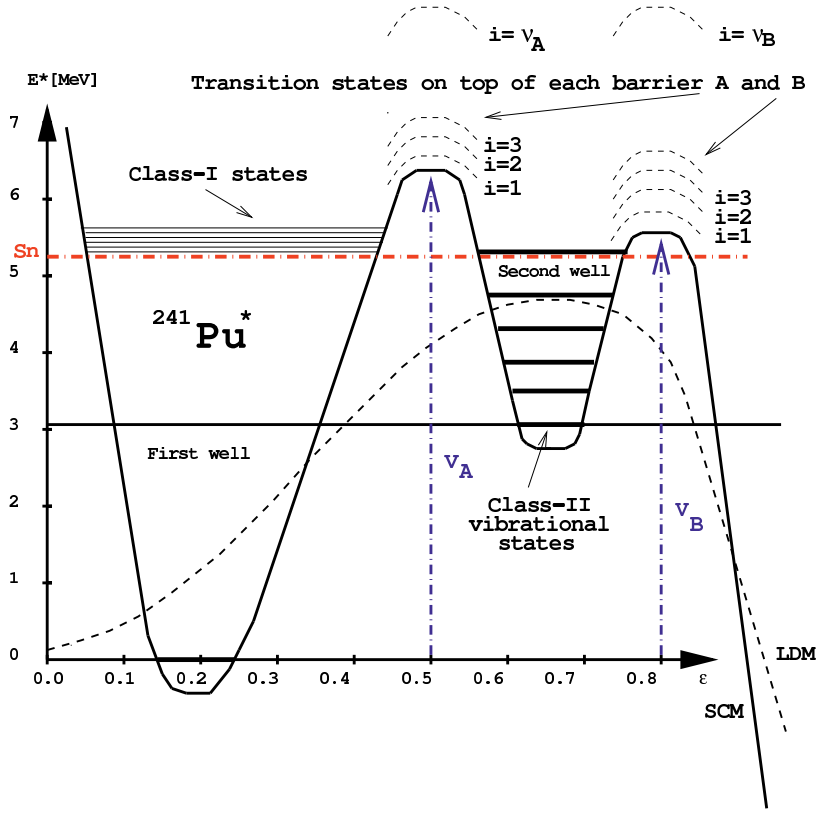

Fig. 1. Schematic representation of the potential energy of deformation of a fissioning nucleus as a function of the elongation. Comparison is made between the single hump of the Liquid Drop Model (LDM) and the double-hump barrier shape of the Shell Correction Method (SCM). The macroscopic contribution provides the overall shape and magnitude of the fission barrier while microscopic corrections lead to the well known formation of a second well along the main deformation axis.

2.3 The impact of the Double Humped Fission Barrier.

The deformation energy of the nucleus involves the changing energy levels of the single nucleons as well as the gross properties such as surface tension and coulomb energy. Strutinsky [7] showed how the 'quasi-magic' effects in the grouping of nucleon levels at certain deformations could have marked effects on the overall energy of the nucleus as a function of deformation. In particular, these effects give rise to a double maximum (or even more complicated form) in the prolate deformation energy of the actinides (see Fig. 1). His theory explained the spontaneously fissioning isomers with relatively low spin (at excitation energies well above the normal spin isomer range) in this group of nuclides as well as striking intermediate structure in their fission cross-sections.

The intermediate structure has major implications for the Hauser-Feshbach formalism. At the 'macroscopic' level the fission transmission coefficient T_f can be modified by the statistical argument of Bjørhnolm and Strutinsky [8], which sees the system as traversing the inner barrier A with transmission coefficient T_A , equilibrating within the secondary well II and either returning through the inner barrier or traversing the outer barrier B with transmission coefficient T_B , and then going on irrevocably to fission. The fission transmission coefficient is then derived as

$$T_f = T_A T_B/(T_A + T_B). \tag{1}$$

This modification is very suitable for excitation energies much higher than the barrier, when many transition states are fully open, but even then requires refinement when the microscopic implications of the double-humped barrier (i.e. the intermediate structure resonances) are taken into account.

2.4 Formal description of intermediate structure.

The cross-sections with intermediate structure effects can be well described within the framework of R-matrix theory. The development here is based on the framework of theory set up in references [9, 10]. In this, the internal nuclear region is explicitly extended to include the deformation through the saddle points of the double-humped barrier towards fission. The channel boundary for this degree of freedom is set at the outer barrier and channels are defined there for each transition state in the spirit of Aage Bohr. The Hamiltonian for the internal system can be written as the sum of a component, which includes the double-humped barrier as the potential energy term (see Fig. 1), for the prolate deformation, one for the other ('intrinsic') degrees of freedom and a mixing (or coupling term) between the two. Suitable boundary conditions are imposed at all the channel boundaries so that the solutions to the Hamiltonian are a set of discrete eigenstates. It can be seen that the wavefunctions of the first component (the so-called vibrational wavefunctions) have the feature of either large amplitude in the primary well (I) and small amplitude in the secondary well (II) or vice versa. The first type are classified as class-I vibrational states and the second as type II. We can now set up a set of class-I compound states by combining the solutions of the intrinsic component with the class-I vibrational states and mixing them by including the coupling term in the diagonalization of the sub-Hamiltonian matrix thus defined. Similarly, we can define a set of class-II compound states.

At this point we mention some basic properties of the class-I and class-II compound states. First, because the only wave-function components that will carry significant deformation amplitude at the outer barrier are the highest energetically available class-II vibration states only the class-II compound states will have a fission width. Second, because the class-II compound states carry no ground state deformation amplitude (in the primary well) they have no neutron width. Thirdly, the radiation widths of the two classes are quite different. The class-II state will only de-excite to states in the secondary well, the cascade terminating at the spontaneously fissioning isomer, and the radiation width magnitude can be different from the that of the class-I states. Without some mixing with the class-I compound states the class-II states cannot show up in the cross-sections of a nucleus in its ground state. Similarly, the class-I states will have no fission cross-section.

The two sets of compound states together must be diagonalized to give a final set of compound R-matrix states that reveal the fission cross-section, using the coupling matrix elements connecting basis states with class-I vibrational components to those with class-II vibrations. At sub- or near barrier energies these matrix elements are very small owing to the very small overlap between the two classes of vibration. Therefore, there are relatively simple solutions to this final diagonalization.

Because the secondary well is some 2 to 3 MeV shallower than the primary well, the class-II compound states are much less dense than the class-I states at a given excitation energy. This allows the study of the mixing of a single class-II state with its many class-I neighbours as a very good approximation at sub- or near-barrier energies. This case can be solved exactly. In the special case of uniform widths and coupling matrix elements of the class-I states, the solution shows that the spreading of the class-II fission width into the final compound states is Lorentzian in form. Its width is proportional to the ratio of the squared coupling matrix element $|\langle \lambda_I | H_c | \lambda_{II} \rangle|^2$ to the level spacing D_I of the class-I states. From this ratio we define the class-II state coupling width

$$\Gamma_{\lambda_{II}c} = 2\pi \, |\langle \lambda_I | H_c | \lambda_{II} \rangle|^2 / D_I. \tag{2}$$

If the coupling width is much larger than the class-II state fission width this Lorentzian expression is a good approximation to the fission widths of the final fine structure resonance states. However, if the class-II fission width is of similar magnitude or much greater than the coupling width then we still have to take into account that these are the R-matrix state properties and we still have to connect the internal nuclear region to the channels to obtain the collision matrix. When the R-matrix state channel widths are large compared with the level spacing this connection can cause a large difference between the widths of the collision matrix poles, which give the cross-section properties directly, and those of the R-matrix states. Thus we find the approximate expression for the fission widths of the poles (ignoring complex phase factors) is

$$\Gamma_{\lambda f} = \frac{D_\lambda}{2\pi} \frac{\Gamma_{\lambda_{II}c}\Gamma_{\lambda_{II}f}}{(E_\lambda - E_{\lambda_{II}})^2 + \left(\Gamma_{\lambda_{II}c} + \Gamma_{\lambda_{II}f}\right)^2/4} \tag{3}$$

The level spacing D_λ is approximately the class-I level spacing. With these fission width parameters inserted into the Breit-Wigner single-level formula for the fine structure resonances we obtain the cross-section through the intermediate resonance. This clustering of the fission width into narrow regions necessarily reduces the average fission cross-section. Averaging over the resonance profile, with the superposition of similar profiles from the full sequence of class-II states added, gives the Back-Lynn expression [11] for the average fission cross-section. We denote this average by $\sigma_{IS,un}$, the "un" subscript denoting that it is derived for uniform class-II and class-I level parameters. The Back-Lynn formula is very different in form from the Hauser-Feshbach formula at near-barrier energies and below, although it does give the same result asymptotically at well above the barrier.

2.5 The effect of level width fluctuations.

Although the class-II level density is much smaller than the class-I density, at neutron separation energies and above it is still sufficiently high to be well within the 'quantum chaos' regime and we can expect large fluctuations in the coupling and fission widths from level to level. A quantitative assessment depends on the number of channels (transition states) open or partially open at the outer barrier and inner barrier. The concept of channels at the fission barrier was well established by Aage Bohr for single hump barrier and applies immediately to the outer barrier. We have shown that the same concept can be applied in the statistical sense to the inner barrier and the expression for the coupling width in terms of the coupling matrix element given above can be broken up into a sum of partial coupling widths for the transition states at the inner barrier. The widths of these channels are uncorrelated and will each have a Porter-Thomas distribution associated with it.

We first consider the effect on the statistical model modification of the fission transmission coefficient (eq. 1) in the Hauser-Feshbach formula. Equation 1 can also be derived from the microscopic theory. But this derivation shows that the rhs of (1) needs to be averaged over the class-II width fluctuations. This results in the multiplication of the rhs of (1) by a Dresner-type integral, which we denote by S_{II}. Thus, in the high energy regime, we can use the Hauser-Feshbach theory with the Bjørnholm-Strutinsky fission transmission coefficient (1) modified by S_{II}, and the fine structure fluctuation factor S_I applied in the usual way. At lower energies the Back-Lynn formula looks intractable to the fluctuation averaging treatment that can be applied to the Hauser-Feshbach formula, but we note that the asymptotic equivalence well above barrier of B-L to H-F implies that the approximation

$$\sigma_{nf} = \sigma_{UN,is} S_I S_{II} \tag{4}$$

is useful at lower energies.

For the most accurate treatment of the sub- to near-barrier regime, however, we use a Monte Carlo treatment of Eq. 3 that includes the fluctuations of both class-II and class-I levels. We carry out a large number of trials, in each of which we select a coupling matrix element for each significant inner barrier transition state from the mean square matrix element as calculated from the inner barrier transmission coefficient for that transition state. The selection is done by the use of pseudo-random numbers to draw from a zero-mean gaussian distribution, thus ensuring that the squared matrix element is drawn from a Porter-Thomas distribution. We do the same for the outer barrier channels. The coupling matrix elements thus selected give the mean coupling width for that particular class-II state, and from them we select the matrix elements for individual class-I states, and thus, on using Eq. 3, obtain the individual resonance fission widths. We also select the reduced width amplitudes for elastic and inelastic neutron widths from appropriate gaussian distributions. Class-I and class-II individual level spacings are selected taking into account the form of their statistical distributions including long-range fluctuations. The partial widths for each individual resonance are then used to give the average contribution

to the average cross-sections from that resonance. After many trials reasonably accurate estimates of the overall average cross-sections are obtained.

Comparison of the results of the Monte Carlo treatment with Eq. 4 for several cases indicates that the Monte Carlo treatment gives fission cross-section values that are up to 25% lower than the approximate analytic values. Overall, taking account of both intermediate structure and width fluctuations of all kinds lowers the estimated fission cross-section for given barrier heights by large amounts. In practice, using the exact treatment can lower the barrier height derived from the analysis of experimental data by up to one half MeV.

In the central part of our work, the creation of an efficient code AVXSF to obtain fission and related cross-sections using the best physics understanding available, the dual analytical and MC approaches have been followed for calculating the most accurate average cross-sections for each partial wave versus excitation energy. The calculation of the S_I and S_{II} fluctuation integrals was usually carried out by numerical quadrature or analytically in certain special cases. At sub-barrier energies the Back-Lynn formula modified by fluctuation integrals is automatically used but is superseded by the MC calculation when the number of open channels (including inelastic neutron channels) is not prohibitively great.

3 Preliminary Results

3.1 Model Parameters

3.1.1 Fission Barriers

The present work is based on one-dimensional barrier penetration theory which well-known approximated results due to Hill and Wheeler [5] assume inverted parabolic barriers. The associated parameters are usually derived from experimental observations and theoretical assessments. Table 1 displays our preliminary parameters, while Figs. 2 and 3 compare barrier heights with those supplied by Bjørnholm and Lynn [10], Möller *et al.* [12], and alternatively compiled in the RIPL-3 database [13]. This latter includes two sets of fission barrier heights, one determined empirically by V. Maslov [14] from experimental fission cross sections near threshold, and another based on Hartree-Fock-Bogolyubov calculations by S. Goriely [15].

Table 1. Fission barrier parameters used for all Pu isotopes examined in this work. All values are in MeV.

Fissioning isotope	V_A	$\hbar\omega_A$	V_B	$\hbar\omega_B$
^{237}Pu	5.60	0.99	4.95	0.40
^{238}Pu	5.65	1.05	5.45	0.60
^{239}Pu	6.15	0.99	5.50	0.40
^{240}Pu	5.65	1.05	5.23	0.60
^{241}Pu	5.93	0.85	5.65	0.40
^{242}Pu	5.40	1.05	5.30	0.60
^{243}Pu	5.92	0.85	5.40	0.55
^{244}Pu	5.30	1.05	5.25	0.60
^{245}Pu	5.60	0.80	5.08	0.40

Straightforward comments can be made from these Figures. The overview of our results shows well their compatibility with those from literature. Although the heights obtained in the HFB calculations for both barriers are consistent with our results in the case of the lower fissioning nucleus mass numbers, they are systematically higher from mass number ”240”. This latter trend is also verified when comparing to the theoretical calculations by Möller *et al.* [12]. But the most relevant tendency shows up in terms of long-range variation over the whole set of mass numbers. The results from both microscopic calculations by S. Goriely [15] and macro-microcopic calculations by Möller *et al.* [12] increase smoothly with the increase of the fissioning system mass number whereas our barrier heights follow an odd-even character-type. The so-called ”empirical” height data extracted by V. Maslov [14], which are of evaluated-type as well, are much more consistent with our results.

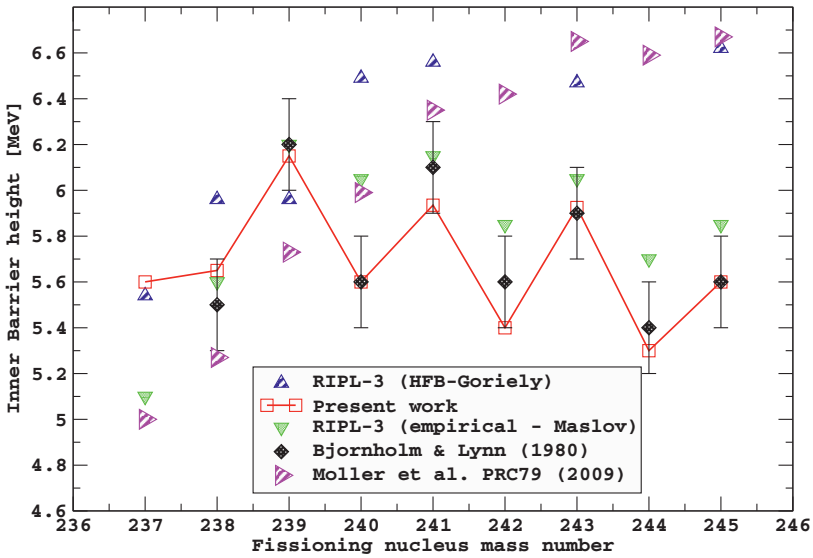

Fig. 2. Systematics of Pu fission inner barrier heights extracted from this work, and compared with previous estimations from Bjørnholm and Lynn [10], theoretical calculations by Möller *et al.* [12] and the values reported in the RIPL-3 database [13].

3.1.2 Individual and Continuum States

At low excitation energies above fundamental barriers in the fissioning systems, dedicated sequences of individual transition states were established during this study. Similarly, sequences of low-lying states were set up for the target nuclei. Data consistency was insured among all compound nucleus systems ruled by their even-even or even-odd characteristics. Indeed the former characteristic implies only collective states at low energy rather than even-odd systems require the introduction of low energy quasi-particle intrinsic states. The construction of the individual state sequences has been already described in Ref. [16] and will not be commented in these proceedings. However we want to recall that a good agreement between experimental and simulated fission cross sections at low neutron incident energies is strongly dependent on the individual sequences finally adopted.

Approximatively 1 MeV above the onset of each individual states sequence, a combinatorial procedure is adopted to construct level densities as a function of the excitation energy and the nucleus deformation. This procedure is a generalization of the method used for creating the individual state sequences and deals with multi-combinations of neutron and/or proton quasi-particle states (leading to 1qp, 3qp, 5qp, etc. or 2qp, 4qp, 6qp, etc. states) and multi-combinations of mass asymmetry, bending, gamma, etc. vibrational states. Subsequent combinations of these multi-quasi-particle and multi-vibrational states are made to form the combinatorial rotational band heads. Other sensitive ingredients of this procedure are the values of the neutron (Δ_n) and proton (Δ_p) pairing gaps at the Fermi energy and those of the moments of inertia $\hbar^2/(2\Im)$, all deformation dependent.

3.1.3 Nucleon Pairing Gaps

Figure 4 plots the neutron and proton pairing gaps extracted from this work versus compound nucleus mass number at the normal, inner and outer barrier deformations. Pairing gap values reflect the differences in the weight of individual states and level densities on top of the pairing condensates and so, are strongly dependent on the broken symmetries of the nucleus at a particular point in the configuration space. Various nuclear structure calculations, e.g., the Hartree-Fock-Bogolyubov calculations with the

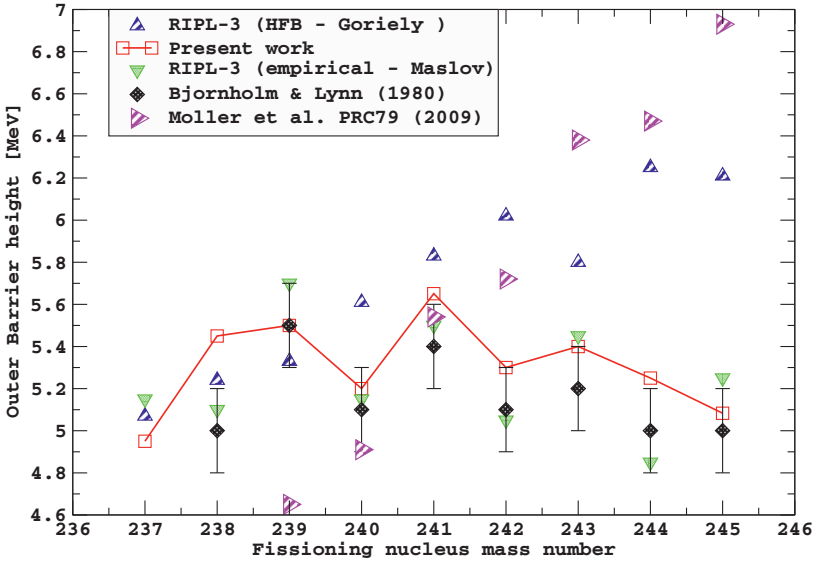

Fig. 3. Systematics of Pu fission outer barrier heights extracted from this work, and compared with previous estimations from Bjørnholm and Lynn [10], theoretical calculations by Möller *et al.* [12] and the values reported in the RIPL-3 database [13].

Gogny force by Delaroche *et al.* [17] or the macro-microcopic calculations by Möller *et al.* [12], indicate that the nucleus deviates from axial symmetry at the first saddle point, but recovers it at the outer saddle while exhibiting mass-asymmetric shapes or octupole deformations. Therefore we logically note that our nucleon pairing gap values at barrier deformation are larger than those extracted at normal deformation. This correlates with odd-even difference in barrier heights since the final agreement between fission cross section and experimental data rely on the balance between barrier heights and level densities.

3.2 Multiphase Temperature Level density

Our analysis of (n,f) cross-section data extends from a few keV up to 5.5 MeV, i.e. just below the onset of second-chance fission. When the excitation energy increases, the level density of the transition states becomes the crucial factor in the accurate determination of the cross-sections. We use our parameterized quasi-particle-vibration-rotation combinatorial model, described in Ref. [16], for both the inner fission barrier and target nucleus level densities whereas a multiphase-nuclear-temperature level density model was used for the outer barrier to allow better agreement between experiments and theoretical calculations. However the choice of such an empirical level density can be justified by the following argument. Standard empirical level density formulae employed at given barrier deformation (main β axis) are excitation energy dependent (i.e.; $\rho(U)$) but no special grant is made for sudden changes in the number of degrees of freedom in the fissioning nucleus leading to sudden symmetry changes. Our fitted multiphase level density, $\rho(U,T)$ -Eq. 5-, by using a constant but independent nuclear temperature (T) in each phase, is willing to cope with this argument.

$$\rho_i(U,T_i) = C_i\ exp(U/T_i) \text{ with } C_i, \text{ constant parameter, over phase } i. \tag{5}$$

Figure 5 shows the behavior of the 15-phases level density adopted for the ^{240}Pu fissioning nucleus on top of the barriers. A same total level density can be reproduced with our quasi-particle-vibration-rotation combinatorial model using two different sets of nucleon pairing gaps, which fitted (Δ_p; Δ_n)

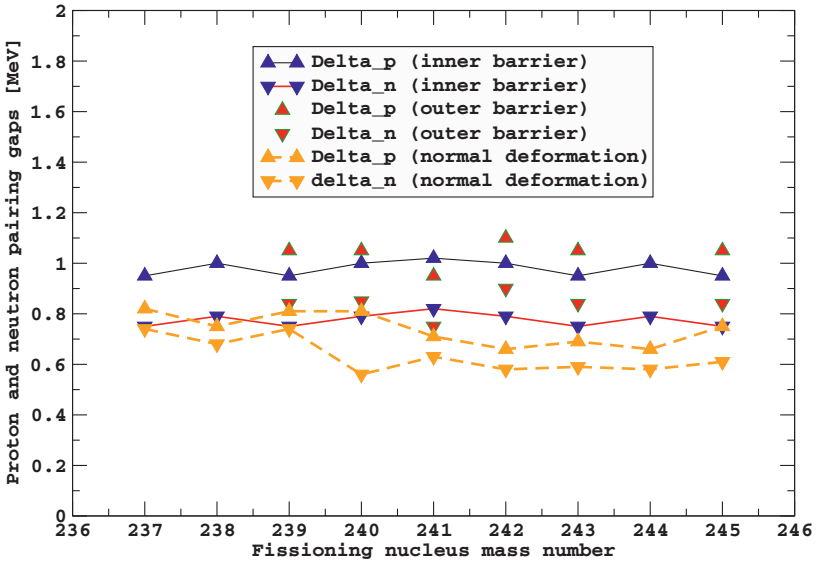

Fig. 4. Systematics of Pu neutron and proton pairing gaps extracted from this work and corresponding to normal deformation (orange triangles), inner (blue triangles) and outer (maroon triangles) barrier deformations.

couples are respectively assigned to $(1.0; 0.8)$ and $(1.1; 0.9)$ MeV. The first major sharp rise in these combinatorial level densities around 0.8 MeV is associated in the degenerescence of two individual collective band heads of mass asymmetry+bending and octuple vibrational natures respectively. On the same figure, we can visualize the postulated inner barrier combinatorial level density which magnitude, is approximately twice the outer barrier level density magnitude because of the axial symmetry breaking. Because of the total absence of neutron-induced experimental data, the prediction of the average fission cross section of ^{243}Pu is still more difficult to draw. We base our cross-section estimate for this nuclide on the analysis of the ^{242}Pu(t,pf) reaction to obtain valuable barrier heights and on models, level density trends and other quantities determined in analyzing the cross-sections of the other plutonium isotopes. Our predicted subthreshold average fission cross section is about twice the ENDF/B-VII.0 (≡ JEFF-3.1.1) evaluated cross section as can be seen on Figure 8.

4 Fission Cross Section Prediction Capability of Short-Lived Nucleus

We believe that the consistent approach carried out during this work on the suite of the Pu isotopes gives us the opportunity to interpolate or extrapolate barrier parameters to the poorly known nuclei of that series with some reliability. In particular, our study relying on both neutron resonance data and transfer reactions analyses, supplies valuable information on barrier heights even for target nuclides which barriers lie below the neutron threshold energy. Figure 6 shows the inelastic and capture neutron-induced cross sections of ^{236}Pu. A change of 100 keV on those barrier heights has a major impact on the predicted capture and inelastic cross sections whereas no significant change is encountered on the related fission cross section. The experimental database of ^{236}Pu is quite sparse in terms of neutron-induced or transfer reactions because of its short life-time ($\tau_{1/2}$ = 2.86y). Figure 7 shows our simulation compared to other evaluated data. The JENDL-4.0 [18] evaluation is representative of the average trend derived from the experimental data, which uncertainties are quite large below 50 keV but claimed to be smaller than 10% above.

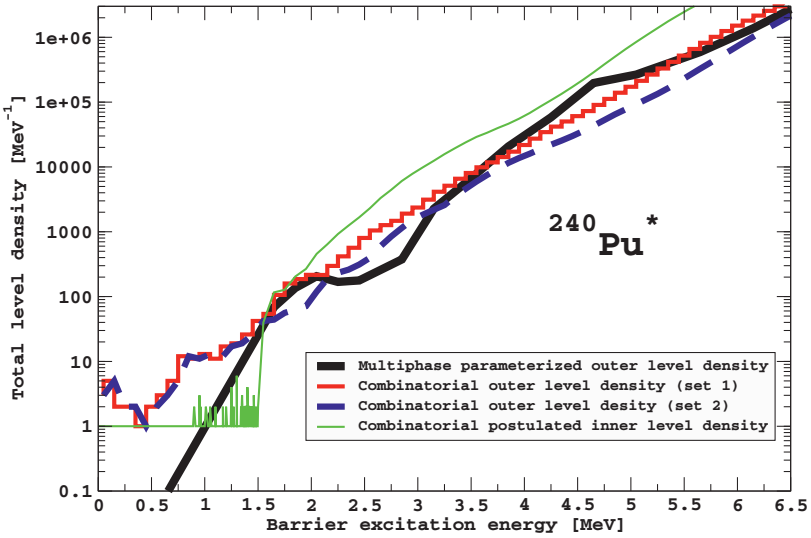

Fig. 5. ^{240}Pu* barrier level densities summed over both parity and all spins versus excitation energy. The black-thick-solid curve is our empirical outer barrier level density (15 constant temperature phases up to 7 MeV barrier excitation energy) fitted to the experimental cross sections whereas both stair-red- and dash-blue curves are based on our combinatorial model for the same density with pairing gap values respectively of Δ_p = 1.0 MeV, Δ_p = 0.8 MeV (set 1) and Δ_p = 1.1 MeV, Δ_p = 0.9 MeV (set 2). The green-thin curve is our postulated inner barrier combinatorial level density superseded below 1.5 MeV by the inner individual transition states sequence.

5 Conclusion and Future Orientations

The *R*-matrix theory applied to the modeling of fission cross sections was developed in the early seventies and carefully used to interpret specific experimental cases of intermediate structures until the end of the eighties. However this is the first time that this theory is used methodically and consistently for a whole isotope family (plutonium) over a broad energy range, from the upper end of the resolved resonances to the onset of second chance fission. Our study demonstrates that a pertinent use of this theory with microscopic input leads to cross section simulations of quality comparable with the existing evaluations in this energy range. It is also shown that extrapolated or interpolated barrier heights and level densities can be used to make reliable cross section predictions for the short-lived isotopes of the series. Eventually for the isotopes whose fission barrier heights lie below the neutron emission threshold, transfer reaction analyses can be exploited to replace neutron resonance spectroscopy data. Ongoing AVXSF developments are focused on a more rigorous treatment of transfer reactions and class-II vibrational states whenever these latter are incompletely damped among the other degrees of freedom. Next stages will involve the other members of the actinide family in order to create a comprehensive "microscopic-type evaluated database" which used in correlation with reference input averaged data will improve our prediction capabilities.

References

1. W. Hauser and H. Feshbach, Phys. Rev. **87**, (1952) 366.
2. C.F. Porter and R. Thomas, Phys. Rev. **104**, (1956) 483.
3. L. Dresner, Proc. Int. Conf. Neutron Interaction, Columbia Univ., CU-**175**, (1957) 71.
4. P.A. Moldauer, Phys. Rev. **123**, 3, (1961) 968.
5. D.L. Hill and J.A. Wheeler, Phys. Rev. **89**, (1953) 1102.

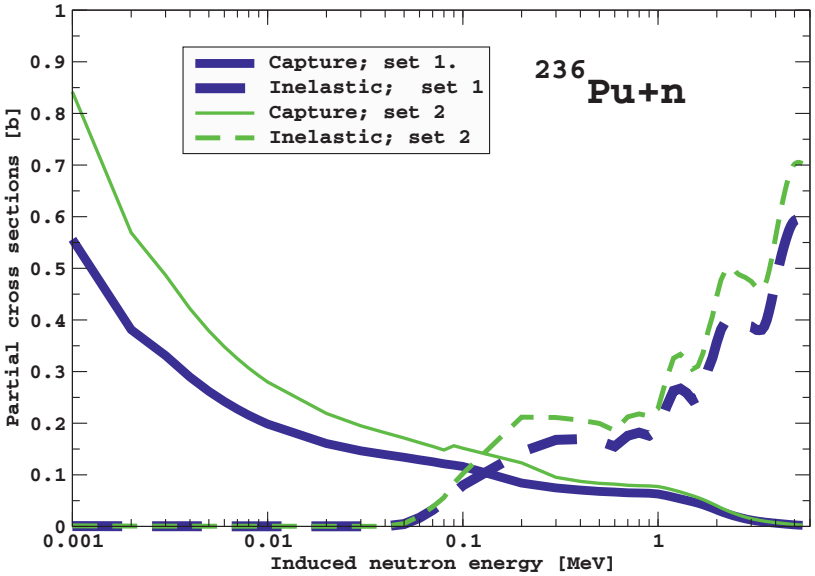

Fig. 6. ^{236}Pu inelastic and capture cross sections versus neutron incident energy computed with our AVXSF code. The blue-thick curves have been established using inner and outer barrier heights respectively equal to 5.6 and 4.95 MeV (set 1) whereas the green-thin curves use barrier parameters shifted 100 keV upwards (set 2).

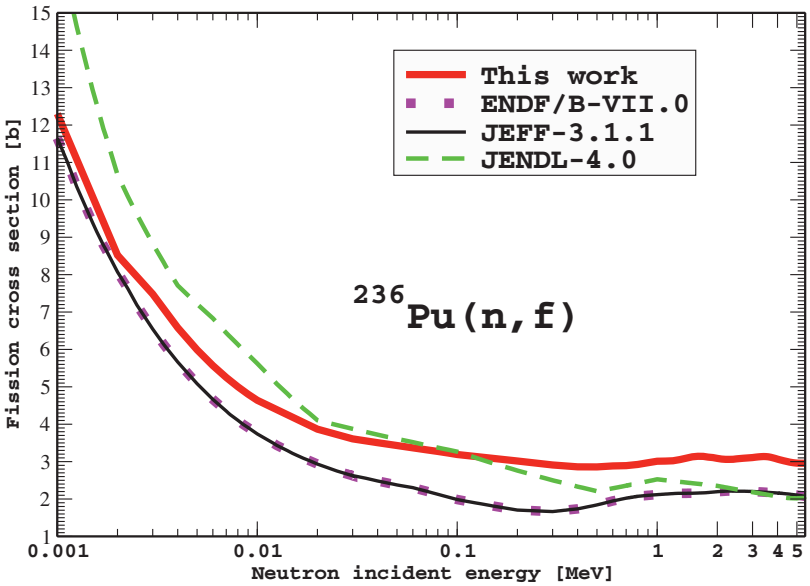

Fig. 7. ^{236}Pu fission cross section (red-solid curve) computed with our AVXSF code versus neutron incident energy and compared to the available evaluated data. Our predicted curve does not trust the average trend given by the experimental data which, are well reproduced by the JENDL-4.0 [18] evaluation.

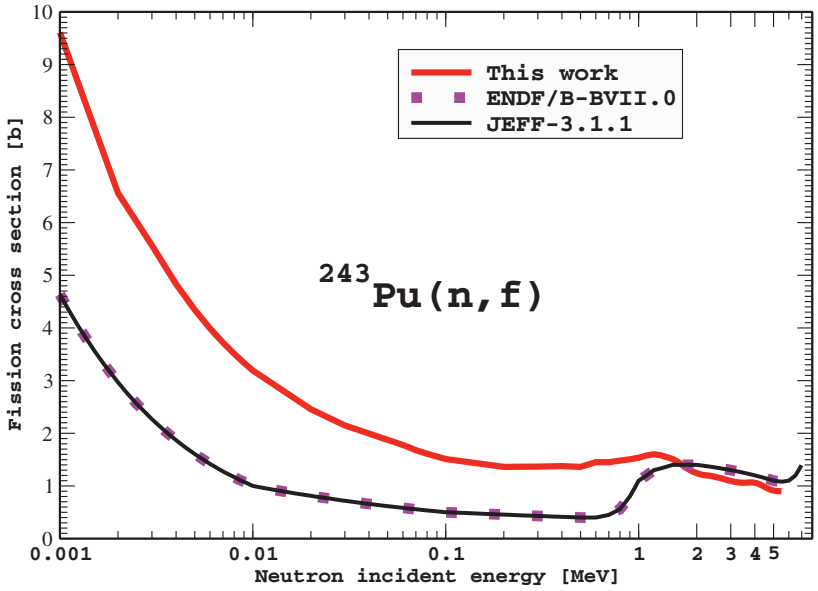

Fig. 8. ^{243}Pu fission cross section (red-solid curve) computed with our AVXSF code versus neutron incident energy and compared to the available evaluated data. Our predicted average fission cross section is twice the value supplied by JEFF-3.1.1 [19] and ENDF/B-VIII.0 [20].

6. A. Bohr, in *Peaceful Uses of Atomic Energy*, Proc. Conf. Geneva 1955, United Nations, New York, Vol.2, p.220 (1956).
7. V.M. Strutinsky, Nuclear Physics A **95**, (1967) 420.
8. S. Bjørnholm and V.M. Strutinsky, Nucl. Phys. **A136** (1969) 1.
9. J. E. Lynn, J. Phys. A: Math. Nucl. Gen., **6**, (1973) 542.
10. S. Bjørnholm and J.E. Lynn. Rev. Mod. Phys. **52**, No. 4, (1980) 725.
11. J.E. Lynn and B.B. Back, J. Phys. A: Math. Nucl. Gen., **7**, No. 3 (1974) 395.
12. P. Möller, A.J. Sierk, T. Ichikawa, A. Iwamoto, *et al.* , Phys. Rev. C**79**, (2009) 064304.
13. R. Capote *et al.*, Nuclear Data Sheets **110**, (2009) 3107.
14. G.N. Smirenkin, IAEA-Report INDC(CCP)-**359** (1993).
15. S. Goriely, S. Hilaire, A.J. Koning, M. Sin, R. Capote, Phys. Rev. C**79**, (2009) 024612.
16. O. Bouland, J. E. Lynn and P. Talou, the European Physical Journal, **2**, (2010) 08001.
17. J.-P. Delaroche, M. Girod, H. Goutte, and J. Libert, Nucl. Phys. **A771**, (2006) 103.
18. K. Shibata, O. Iwamato, T. Nakagawa, *et al.* , "JENDL-4.0: a new library for nuclear science and engineering," J. Nucl. Sci. and Tech., **48**, 1, (2011) 1.
19. A. Santamarina *et al.* , JEFF Report **22**, OECD/NEA (2009).
20. M.B. Chadwick, P. Obložinský, M. Herman *at al.*, "ENDF/B-VII.0: Next Generation Evaluated Nuclear Data Library for Nuclear Science and Technology," Nuclear Data Sheets, **107**, (2006) 2931.